Experimental Study on an SI Engine Mapping Considering Performance, Emissions, and Cyclic variability

Melih YILDIZ[1] ve Bilge ALBAYRAK ÇEPER*[2]

[1] *Iğdır University, Faculty of Engineering, Department of Mechanical Engineering, Iğdır, Turkey, melih.yildiz@igdir.edu.tr*

[2] *Erciyes University, Faculty of Engineering, Department of Mechanical Engineering, Kayseri, Turkey, balbayrak@erciyes.edu.tr*

Özet

The engine manufacturer has aimed to attain optimum values for engines operating different loads and speeds by utilizing the characteristics of both spark-ignition engines having a ready combustion control and compression ignition engines resulting in low emissions, fuel consumption and, a high engine output power for years. In this regard, the efforts on the improvement in engine performance, emissions, and thermal efficiency of the engines have been constantly continuing to be updated for their whole specifically operating range. In this study, a series of experiments was performed to construct the maps of a two-cylinder, four-stroke spark-ignition engine. Considering the engine characteristics at full load, the engine was tested at seventy operating conditions depending on speed and load. With the obtained data, the engine maps were created for performance, emissions, and cyclic variability of maximum pressure, brake mean effective pressure.

Keywords: Spark ignition engine, Engine mapping, Performance, Emissions, Cyclic variability

1. INTRODUCTION

Internal combustion engines use approximately one-third of the Daily total World oil production. With the increase in the number of internal combustion engine vehicles, air pollution has been rapidly increasing due to the emitted emissions into the atmosphere. Therefore, the efforts have been getting great attention to deal with the efficient use of fuel in engines and the reduction of pollutant emissions in exhaust gases [1].

Internal combustion engines are classified as spark ignition (SI) and compression ignition (CI) engines according to their combustion characteristics. A conventional SI combustion can be characterized by the flame formation and the development and spread of this flame. The initiation of the combustion reaction is achieved by controlling the spark plug ignition timing. In compression ignition engines, it starts with the spraying of fuel on the compressed air and self-ignition and continues. In both of these combustion events, the improvement of performance and exhaust emissions depends on efficient combustion in a very short time. Adjusting a large number of parameters according to the operating conditions of the engine to keep the combustion efficiency at the maximum level in all operating conditions of the engine

provide the most efficient conversion of fuel to energy. Fort his purpose, some operating parameters such as ignition timing, valve timings, compression ratio, and air-fuel ratio change depending on engine speed and load [2]. In addition, the researchers investigated different alternative fuel addition to gasoline, and evaluated their effects on engines' performance and emissions. Topgül et al. [3] examined the effects of excess air coeffcients, ignition timings, compression ratio, and inlet air temperature values on exhaust emissions in a single cylinder, four-stroke, spark-ignition engine. They found that the increase in the ignition advance causes the reduction of CO emissions, and the increase in the ignition advance up to 30 ^{o} CA increased HC emissions.

İsmail and Mehta [4] investigated the effects of hydrogen addition to gasoline on engine performance using mathematical modeling. They reported that hydrogen addition to gasoline at different rates had a positive effect on engine performance. Aktaş and Doğan [5] examined the effects of LPG addition to diesel fuel at different rates on engine performance and emissions in a single cylinder, four-stroke CI engine. The used CI engine was operated at the speed where the maximum torque takes place. Besides, diesel fuel was used as pilot fuel and LPG was added into the cylinder in different proportions by weight. They observed that the addition of LPG to diesel caused the decrease in NOx and soot emissions with HC emission penalty. Özer and Vural [6] performed the study to investigate the possibility of acetylene gas as an alternative fuel in a spark ignition engine. They stated that the addition of acetylene by 20% and 30% worsened combustion while different rates of reductions in exhaust gas temperature, HC, CO, CO_2, and NOx emissions were detected.

Literature surveys show that various parameters influence engine performance and emissions. Therefore, it is essential to define the characteristics of any engine operating different load and speed conditions to determine the improvement potential in the engine. In this study, a series of experimental studies were carried out to create the engine maps in terms of performance, emission and cyclic variability.

2. MATERIAL AND METHOD

Experimental studies were carried out on a four-stroke spark ignition Lombardini LGW523 engine at the Engine Laboratory of Mechanical Engineering Department of Erciyes University. The technical specifications of the engine are given in Table 1. The schematic view of the experimental setup is also illustrated in Figure 1.

Table 1. Test engine specifications

Numbers of cyclinder	2
Cylinder volume	505 cc
BorexStroke	72x62 mm
Compression ratio	10.7:1
Max. Power	15 kW
Max.Torque	34 Nm 2150 rpm
Cooling type	water

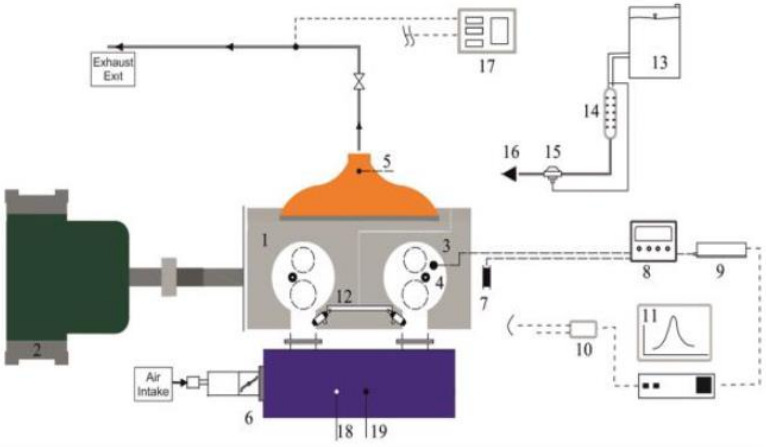

(1)Test engine, (2)dynamometer, (3) in-cylinder pressure sensor,(4)spark plug, (5)exhaust gas temperature-termocouple, (6) throttle (7) encoder, (8) amplifier (9) oscilloscope, (10) data logger, (11) computer, (12) port injector system, (13) fuel tank, (14) scaled container, (15) regülatör, (16) fuel pump, (17) gas emissions device, (18) termocouple for intake air temperature, (19) pressure sensor.

Figure 1. Schematic experimental setup

In the experimental study, a 50 kW hydraulic dynamometer was used to enable the engine to be controlled for different load and speed conditions. With this dynamometer, different speeds and torque can be controlled by adjusting engine load using water brake. Emission measurements were carried out using a Bosch BAE-070 gas analyzer whose technical specifications are summarized in Table 2.

Table 2. Exhaust gas analyzer specifications

Parameter	Range	Unit	Sensitivity
HC	0-20,000	ppm	1.0
CO_2	0-20	%	0.1
CO	0-15	%	0.001
O2	0-21.7	%	0.01
Lambda	0.6-1.2	-	0.001
NOx	0-5,000	ppm	1.0

In-cylinder pressure for combustion analysis was measured using a Kistler 6053CC brand pressure sensor whose specifications are given in Table 3. By setting to a suitable mode and a low pass filter range of 100 kHz to avoid irregularities in the form of signal drift due to noise,

vibration, and thermal shock, the Kistler 5018A brand signal amplifier (Table 4) was used to amplify the signal coming from the pressure sensor. In order to display the signal values in voltage unit, and record these data, Pico branded oscilloscope was used with PicoScope-Automotive software.

Table 3. Pressure sensor specifications

Measurement range	bar	0-250 bar
Calibration interval	bar	0-50, 0-100, 0-150, 0-250
Sensitivity	pC/bar	≈ -20
Natural frequency	kHz	160
Operating temperature range	ºC	-20 ile 350

Table 4. Amplificator specifications

Measurement range	pC	±2 -2.2x10^5
Errors <10 pC <100 pC ≥ 100pC	 % % %	 <±2 <±0.6 <±3
Signal mode	pC/s	<±0.03

A rotary type encoder that generates 3-4 V at each 360º rotation was used to determine the crank angle position. During the experiments, the cooling water temperature was kept at 85 ± 2 ºC.

Exhaust gas temperature was measured in the line close to the oxygen probe, 10 cm from the exhaust manifold. Experimental studies were conducted at seventy operating points specified in Figure 2 by utilizing the engine characteristics at full load conditions.

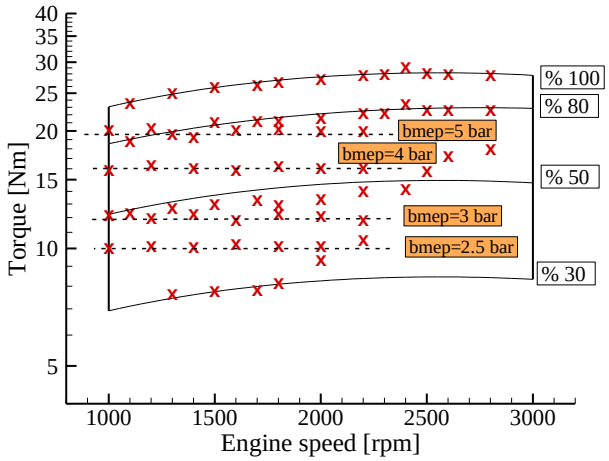

Figure 2.Experimental study points

3. RESULTS

Performance and Emissions

The experiments were commenced with the full load performance test of the engine. With the determination of the engine characteristics at full load, experiments were also carried out for different load conditions, 80%, 50%, and 30% loads at different engine speeds in the range of 1100 to 2800 rpm as shown in Figure 2.

Torque, power, and specific fuel consumption obtained at full load are given in Figure 3. As seen in Figure 3, the maximum torque value was obtained at 2300 rpm about 28 Nm at full load condition. Torque variation tends to decrease after this speed value. Specific fuel consumption, on the other hand, is high at low speeds. With the increase of engine speed,

specific fuel consumption decreases. This is due to the fact that the specific fuel consumption decreases as the amount of increase in power are greater than the amount of fuel increasing per unit of time.

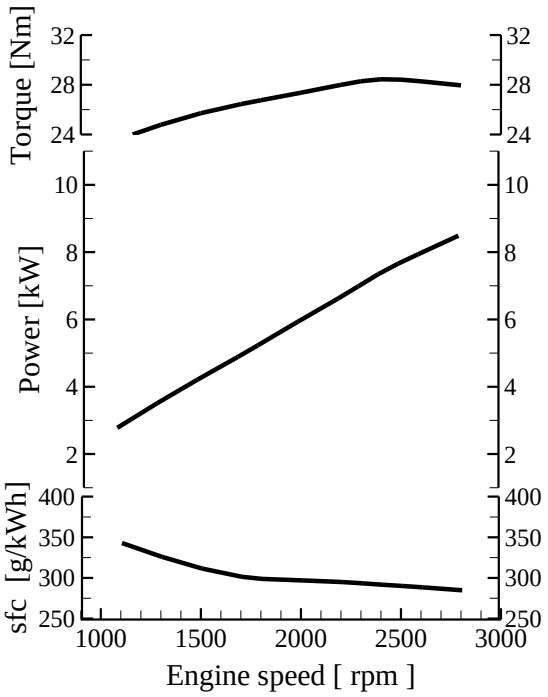

Figure 3. The engine performance characteristics at full load

Figure 4 shows specific fuel consumption variation depending on the engine speed and brake mean effective pressure values. Specific fuel consumption values decrease with the increase of BMEP values, and vary between 297 and 504 g/kWh. The value of BMEP is an average in-cylinder pressure value maintaining the same power value obtained from the related engine cycle, which means BMEP values are relevant to engine load. Therefore, increasing the engine load brings about the engine output power to increase, and the specific fuel consumption values decreased with increasing BMEP values.

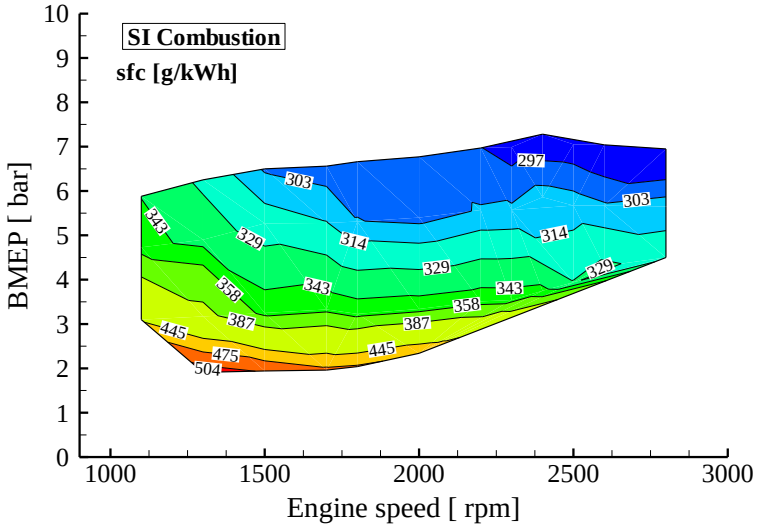

Figure 4. Specific fuel consumption(sfc) map of the engine

Figure 5 illustrates the brake thermal efficiency distribution at different BMEP and engine speeds. As seen in the figure, the distribution characteristic of the thermal efficiencies is similar to that of sfc, but inversely distributed. This is because sfc and thermal efficiency are inversely linear dependent parameters. Therefore, the thermal efficiency values increase at the operating condition where sfc values decrease and vice versa. The brake thermal efficiency values, hence, varied between 0.17 and 0.29 in the tested operating range.

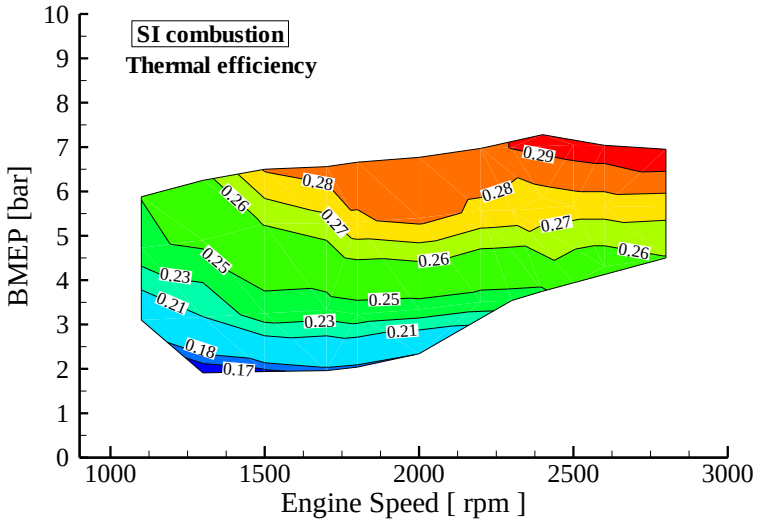

Figure 5. Brake thermal efficiency map of the engine

The major emissions except CO_2 emitted from a SI engine are NOx, HC, and CO. NOx formation generally occurs due to three main factors. The first is thermal NOx formation that occurs in high temperature zones in a cylinder. Another mechanism is prompt NOx formation arising with the rapid reactions especially taking place in the rich mixture zones. Finally, NOx formation is also caused by N_2 molecules contained in the fuel. However, among these mechanisms for the NOx formation, the thermal NOx formation is particularly dominant [7]. Therefore, the exhaust gas temperature values were measured to be able to assess the relationship between NOx formation and exhaust gas temperature values. Figure 6.a shows the variation of exhaust gas temperature values. Exhaust gas temperature goes up when both BMEP and engine speed increase. Furthermore, NOx values as shown in Figure 6.b are directly related to exhaust gas temperature, and both of them have similar distribution trends. This is because exhaust gas temperature values imply what level value of combustion temperature occurs in the cylinder. In addition, exhaust gas temperature and NOx values change remarkably by BMEP rather than the engine speed as understood in Figure 6.a-b.
Figure 6.*c* and *d* show the CO and HC emissions. Although in-cylinder temperature value is a significant factor for CO formation, a fuel-air ratio, homogeneous in a cylinder, dissociation reactions due to high temperature are also key factors. Low temperature zones particularly close to cylinder walls give rise to CO formation by decreasing oxidation from CO to CO_2 . Besides, CO formation is able to be caused by a local rich-mixture zone due to decreasing O_2 concentration [8]. As shown in Figure 6.c, CO emissions is minimum especially at low speeds and high BMEP values. CO emission values reached the maximum values at the engine speed of 2500 rpm and moderate load levels. In general, both BMEP and engine speed parameters do not have a significant effect on the change in CO formation.

HC formation is related to in-cylinder temperature zones, fuel-air mixture ratio, and homogeneity in the cylinder. The lack of O_2 in local rich mixture zones contributes particularly to HC formation. On the other hand, the quite lean mixture zones also cause HC formation due to low temperature and extinguished flame. In addition to these, another factor for HC formation results from the burning of thin film layers formed on the walls of the cylinder [9]. Figure 6.d shows the distribution of HC emission values measured at different BMEP and engine speeds.

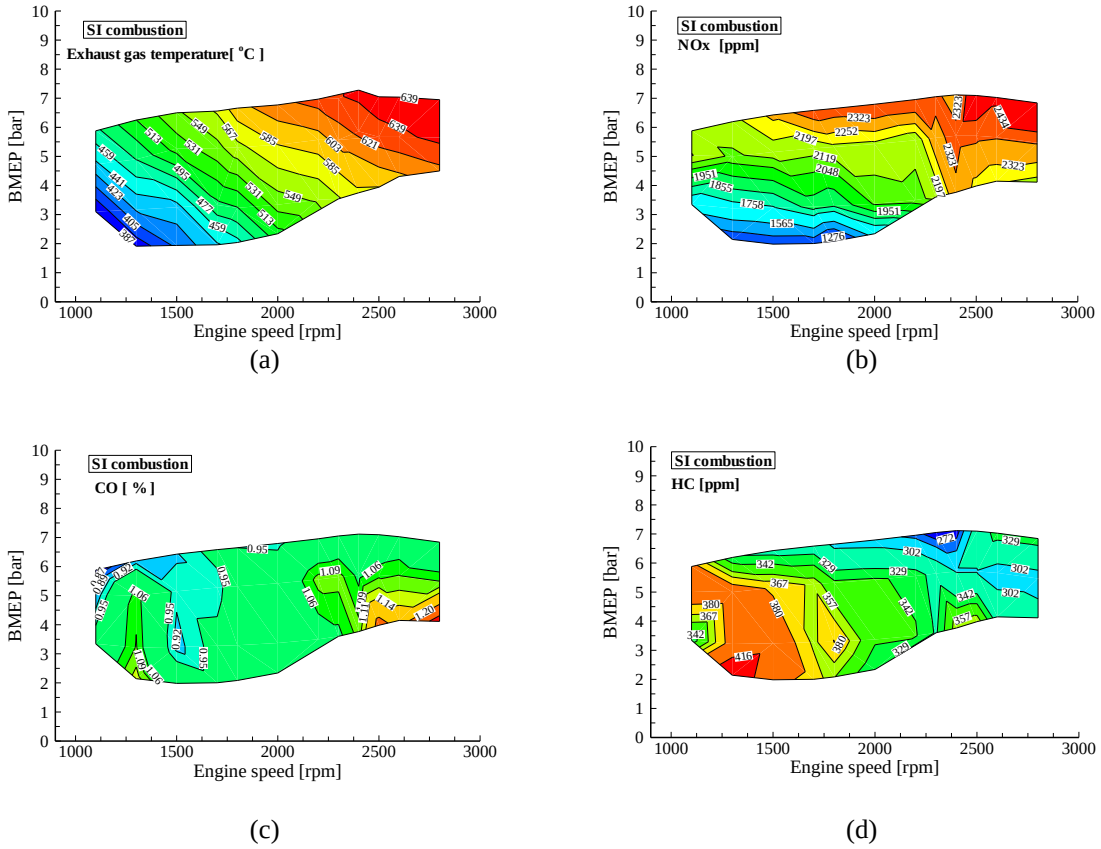

Figure 6. Emissions and exhaust gas temperature (a) exhaust gas temperature, (b) NOx emission, (c) CO emission, (d) HC emission

Combustion Analysis

Figure 7 shows the pressure traces of 300 consecutive cycles and the mean pressure curve representing the engine cycle at the specified operating condition.

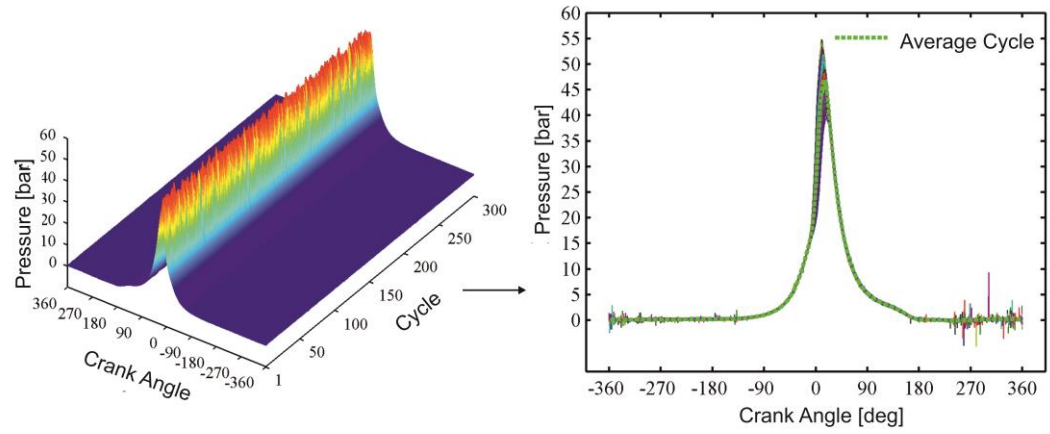

(a) 1500 rpm -100% load

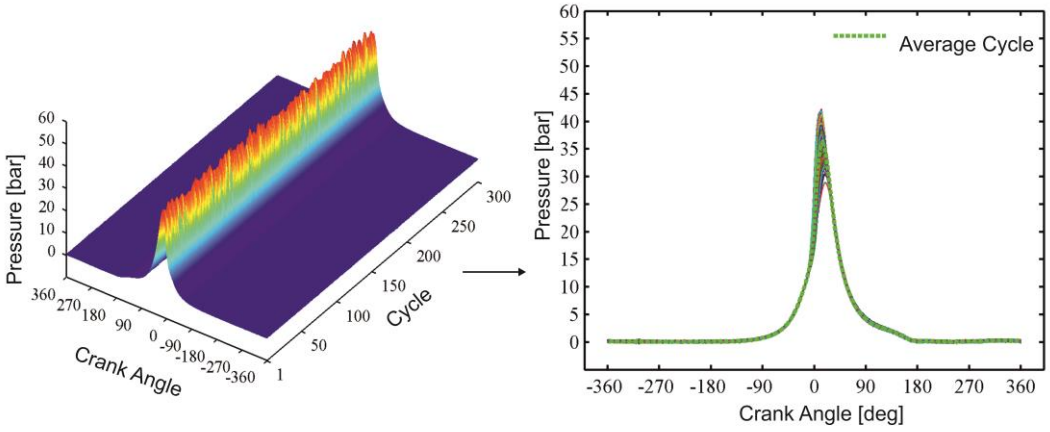

(b) 1500 rpm -80% load

Figure 7. In-cylinder pressure traces

Figure 8 illustrates the pressure traces and corresponding pressure rise rates (PRR) for different loads at the specified engine speeds. As shown in the figure, decreasing operating load caused the peak pressure values to be decreased. Besides, the pressure rise rates decreased when the operating load decreased. The main parameters obtained from these pressure traces are summarized in Table 5.

Figure 9 shows the heat release rate curves for different engine speeds and loads. Heat release rate (HRR) gives the information what rate combustion reaction occurs in an internal combustion engine [10]. As can be seen in Figure 9, the heat release rate decreases significantly with the decrease in the load. The reason for this is that the energy content in the cylinder decrease at a low load.

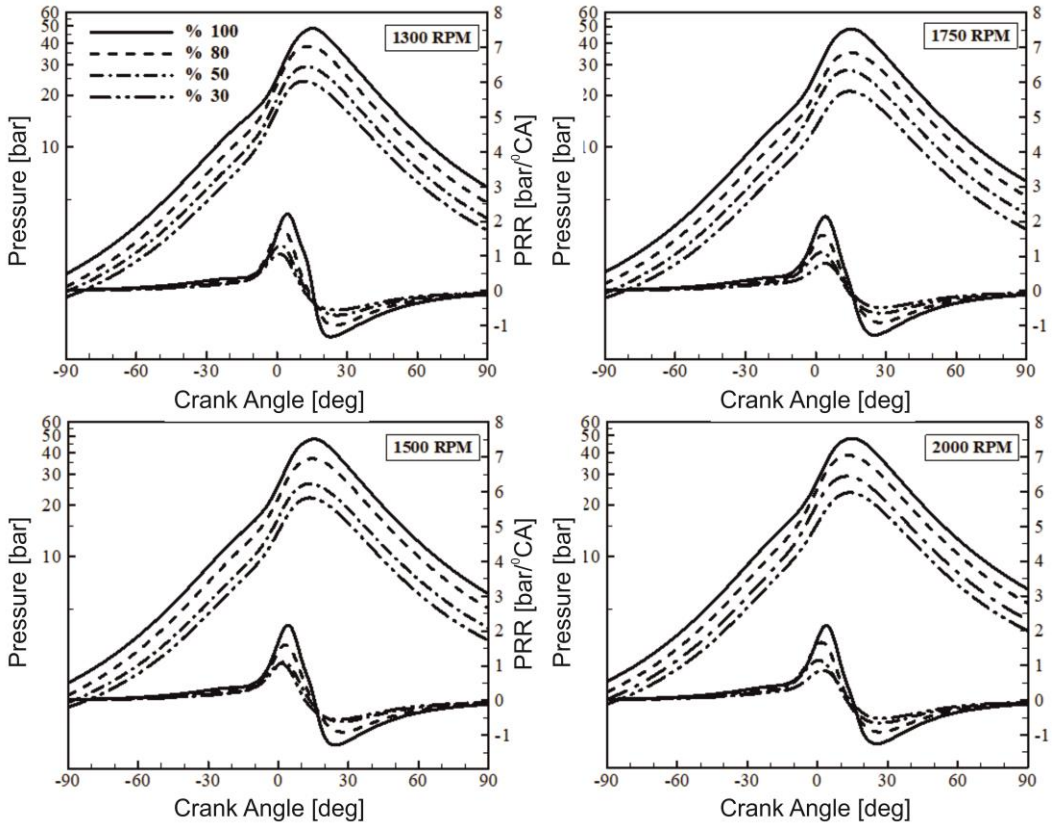

Figure 8. Pressure traces and pressure rise rate(PRR)

Table 5. Maximum pressure, its location, and maximum pressure rise rate

1300 rpm				
Load	**%100**	**%80**	**%50**	**%30**
Pmax. [bar]	48.70	38.11	29.14	24.10
Pmax_loc. [CA]	15.30	13.40	12.50	11.50
(PRR)max [bar/^{o}CA]	2.36	1.88	1.43	1.17
1500 rpm				
Pmax. [bar]	47.90	36.87	26.37	21.92
Pmax_loc. [KMA]	10.90	11.80	15.40	17.20
(PRR)max [bar/^{o}KMA]	2.31	1.71	1.20	0.97
1750 rpm				
Pmax. [bar]	48.15	35.26	27.84	21.06
Pmax_loc. [KMA]	15.30	14.60	13.80	14.50
(PRR)max [bar/^{o}KMA]	2.32	1.55	1.21	0.87
2000 rpm				
Pmax. [bar]	47.20	33.20	26.78	21.58
Pmax_loc. [KMA]	15.70	14.80	13.60	14.60
(PRR)max. [bar/^{o}KMA]	2.21	1.38	1.12	0.87

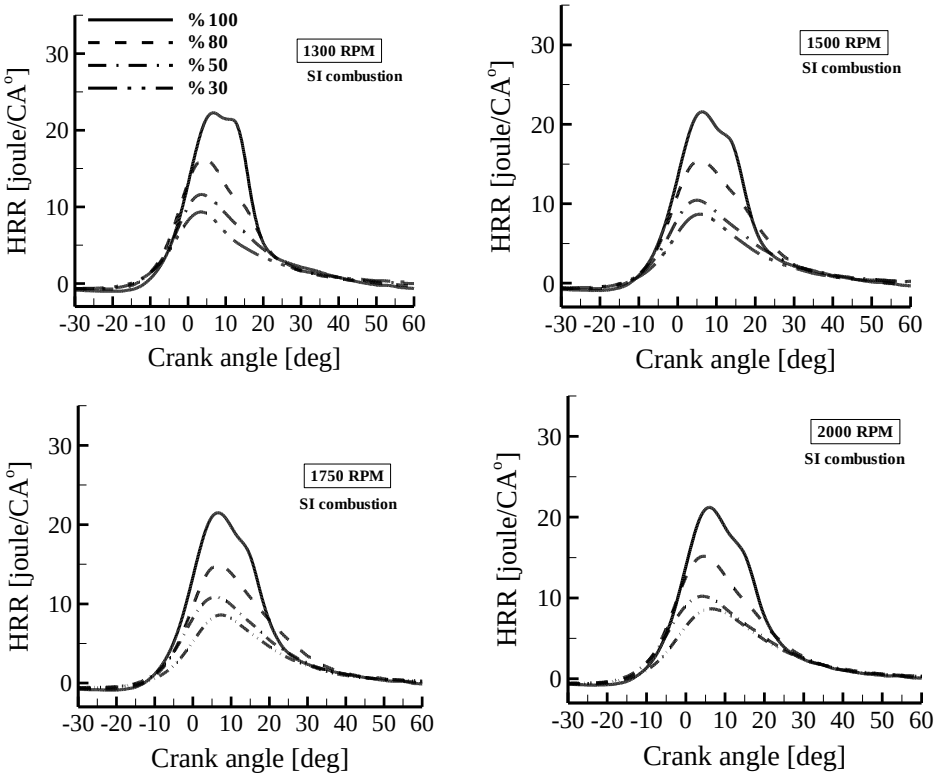

Figure 9 Heat release rate curves at different loads

Another investigation in combustion analysis is the mass fraction burned curves to determine the main combustion phases, CA10, CA50, and CA90 [11]. Thus, combustion duration is able to be determined by utilizing these phases. In general, the Wiebe function and Rassweiler&Withrow methods are used to obtain the MFB curves [11]. Wiebe function is a method used especially in an unpredictive combustion modeling study[12-14]. On the other hand, Rassweiler&Withrow method based on pressure rise due to the change in cylinder volume and combustion is the most commonly used in experimental studies.

CA10, CA50, and CA90 combustion phase locations in which 10%, 50%, and %90 of the fuel mass consumed respectively are the main locations to control combustion development [15]. The combustion duration is, generally, considered as the time between CA10 and CA90. CA50 is significant to control combustion as it is regarded as the point where maximum heat release takes place. Therefore, examining these points in combustion analysis gives important insights into combustion development [17]. Figure 10 shows the mass fraction burned curves obtained by Rassweiler&Withrow method at different loads and engine speeds. As seen in the figure, combustion duration in CA prolongs by decreasing engine load. Besides, CA50 locations for most of the operating conditions are close to each other.

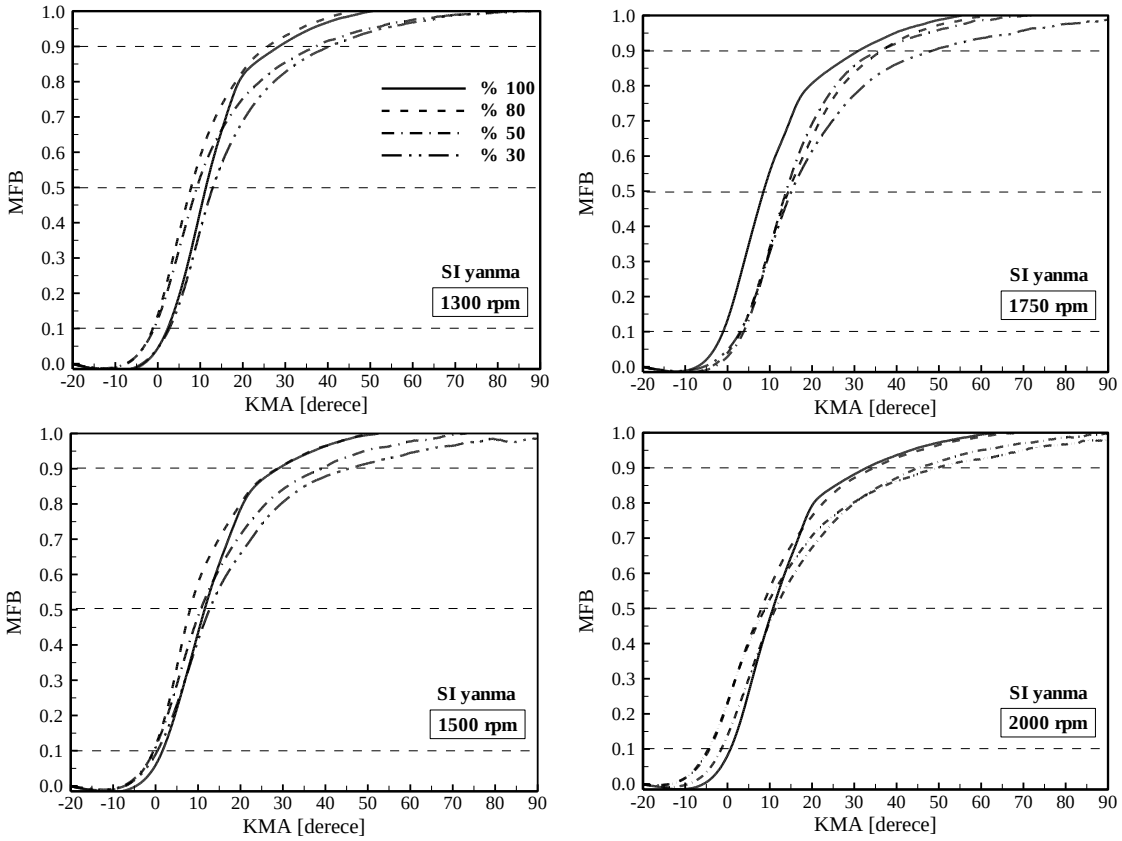

Figure 10. Mass fraction burned (MFB) curves at different loads

Cyclic Variability

The engine stabilization during its running relies on the engine's control systems responding to varying load and speed conditions. The engine stabilization is determined by assessing the cyclic variability [18-22]. Many parameters can be investigated to evaluate cycle to cycle variation such as indicated mean effective pressure (IMEP), maximum pressure, combustion phase locations, etc. But, the cyclic variation of IMEP is a decisive parameter for performance stabilization while maximum pressure cyclic variation is for combustion stability. Figure 11 shows the coefficient of variation of the indicated mean effective pressure (CoVimep). The maximum CoVimep is 1.86% which means a stable operating as the threshold value is up to 5.0% [23]. If the CoVimep value is high, the power generation at each cycle is highly variable, which in turn it means that the engine runs unstable.

Another coefficient of variation is for the maximum pressure values inside the cylinder. This value is especially important in terms of combustion stabilization when it shows the variability of the maximum pressure values reached with heat release. Figure 12 shows the variation of coefficients of maximum pressure (CoVpmax) at different engine speeds and BMEP values. It is seen that CoVpmax values vary between 4.2% and 9.4%, and the engine load rather than the engine speed influences the variation of Pmax values.

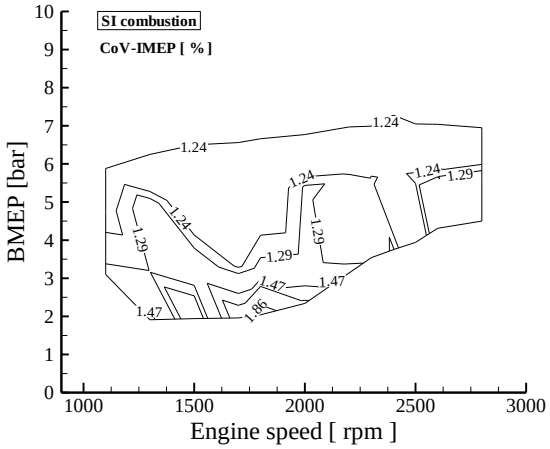

Figure 11 Indicated mean effective pressure coefficient of variation(CoVimep)

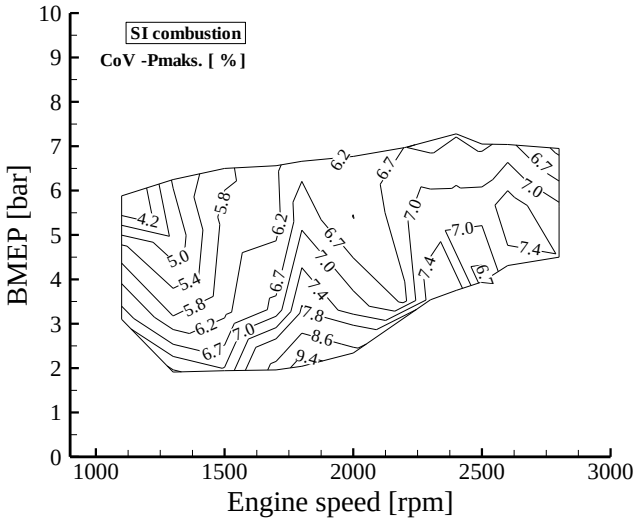

Figure 12 Maximum pressure coefficient of variation(CoVimep)

4. CONCLUSION

The experiments were carried out to determine the characteristics of the engine controlling its electronic control units. This study presented the basic parameters of the engine's characteristics over the map graphs to reveal the improvement potential in the engine for future studies.

REFERENCES

[1] Çırak B., Gürbüz H., Yapay sinir ağları kullanarak dizel motorlarda termal bariyer kaplamanın emisyonlara etkilerinin incelenmesi, Nevşehir Üniversitesi Fen Bilimleri Enstitüsü Dergisi 1, 24-35, 2012.

[2] Sekmen Y., Erduranlı P., Gölcü M., Salman M.S., Buji ile ateşlemeli motorlarda sıkıştırma oranı değişiminin performans parametrelerine etkisi, Pamukkale Üniversitesi Mühendislik Bilimleri Dergisi, 11(1), 23-30, 2005.

[3] Topgül T., Yücesu H.S., Okur M., Buji ile Ateşlemeli Bir Motorda Çalışma Parametrelerinin Egzoz Emisyonlarına Etkilerinin Deneysel Olarak İncelenmesi, Politeknik Dergisi, 8(1),43-47, 2005.

[4] Saleel I., Mehta P. S., Second Law Analysis of Hydrogen Air Combustion in a Spark Ignition Engine, International journal of hydrogen energy, 36 (1): 931-946, 2011.

[5] Aktaş A., Doğan O., Çift Yakıtlı Bir Dizel Motorda LPG Yüzdesinin Performans ve Emisyonlara etkisi, Gazi Üniversitesi Mühendislik Mimarlık Fakültesi Dergisi, 25 (1):171-178, 2010.

[6] Vural E., Özer S., Buji ateşlemeli motorlarda yakıta asetilen gazı ilavesinin egzoz emisyonlarına etkisinin deneysel analizi, BEU Fen Bilimleri Dergisi 3(1), 24-34, 2014.

[7] Albayrak Ç. B, Yıldız M, Akansu S.O, Kahraman N. Performance and emission characteristics of an IC engine under SI, SI-CAI and CAI combustion modes, ENERGY, Vol. 136, p. 72-79, 2017.

[8] Canakcı M. An experimental study for the effects of boost pressure on the performance and exhaust emissions of a DI-HCCI gasoline engine. Fuel 2008(87):1503-14.

[9] Heywood, J.B. 1988. Internal Combustion Engine Fundamentals, McGraw-Hill, New York

[10] Yıldız, M., Akansu, S.O, Çeper, B.A. Computational study of EGR and excess air ratio effects on a methane fueled CAI engine. International Journal of Automotive Engineering and Technologies. 2015, (4);3:152-161.

[11] Stone R. Introduction to Internal Combustion Engines, Third Edition. Society of Automotive Engineers Inc. Warrendale, 1999.

[12] Yıldız, M., Albayrak Çeper, B. Zero-dimensional single zone engine modeling study on methane-fueled SI engine using single and double Wiebe functions, 9 th Sustainable Energy and Environmental Protection, Kayseri, Türkiye, 22-25 Eylül 2016, pp.208-215

[13] Yeliana, Y., Cooney, C., Worm, J., Michalek, D.J, Naber, J.D. Estimation of double-Wiebe function parameters using least square method for burn durations of ethanol-gasoline blends in spark ignition engine over variable compression ratios and EGR levels. Applied Thermal Engineering, 31(2011): 2213- 2220.

[14] Mittal M, Schock H. Fast mass-fraction-burned calculation using the net pressure method for real-time applications. Proceeding of the Institution of Mechanical Engineers, Part D: Journal of Automobile Engineering, 2008(223):389-394.

[15] Hunicz, J.,Kordos, P. An experimental study of fuelinjection strategies in CAI engine, Experimental Thermal and Fluid Science, 35(2011):243-252.

[16] Zhao H. Motivationdefinitionandhistory of HCCI/CAI engines. In: Zhao H, editor. HCCI and CAI Enginesforthe Automotive Industry, Woodhead Publishing Limited, 2007.

[17] Maurya, R.K, Agarwal, A.K. Experimental investigation on effect of intake air temperature and air-fuel ratio on cycle-to-cycle variations of HCCI combustion and performance, Applied Energy, 2011(88)1153-63.

[18] Kım, D.S, Kım M.Y, Lee, C.H. Combution and emission characteristics of partial homogeneous charge compression ignition engine. Combust. Sci. and Tech. 177(2005):107-125

[19] Lee,C.H.,Lee K.H. An experimental study of the combustion characteristics in SCCI and CAI based on direct injection gasoline engine. Experimental Thermaland Fluid Science, 31(2007):1121-32.

[20] Chen, T.,Xie,H.,Li,L.,Zhang,L., Wang,X., Zhao, H. Methods to achive HCCI/CAI combustion in 4VVAS gasoline engine, Applied Energy. 116(2014)41-51.

[21] Li,h.l.,Neil,W.S., Chippor, W. CycletocycleVariation of a HCCI engine operatedwith n-heptane. Spring Technical Meeting CombustionInstitute/CanadianSection,Paper 5;1-6,2007

[22] Choi,S.,Park,W.,Lee,S.,Min,K.,Choi,H. Methods for in-cylinder EGR stratification and its effects on combustion and emission characteristics in a diesel engine, Energy, 36(2011):6948-59.

[23] Osborne, R.J., Li, G., Sapsford S.M., Stokes, J., Lake, T.H. Evaluation of HCCI for future Powertrains. SAE paper, 2003-01-0750.